

# PROGRADE AND RETROGRADE TERMS OF GRAVIMETRIC POLAR MOTION EXCITATION ESTIMATES FROM THE NEWEST GRACE GRAVITY FIELD MODELS

J. ŚLIWIŃSKA, J. NASTULA

Space Research Centre, Polish Academy of Sciences - Poland  
jsliwinska@cbk.waw.pl, nastula@cbk.waw.pl

**ABSTRACT.** In this study, we computed hydrological polar motion excitation functions (Hydrological Angular Momentum, HAM) from two recent releases of GRACE (Gravity Recovery and Climate Experiment) monthly gravity field models, RL05 and RL06. In contrast to the previous works, here, the equatorial components of polar motion excitation functions ( $\chi_1$  and  $\chi_2$ ) were decomposed into prograde ( $\chi_P$ ) and retrograde ( $\chi_R$ ) time series by applying Complex Fourier Transform (CFT). The computed series were evaluated by comparison with the hydrological signal in observed polar motion excitation (geodetic residuals, GAO). We examined temporal variations of HAM series in seasonal and non-seasonal spectral bands. We showed that both  $\chi_P$  and  $\chi_R$  terms of HAM can be determined by GRACE satellites with congruous levels of accuracy. We also demonstrated that the new GRACE RL06 data increased the consistency between solutions from different data centres and improved the agreement between GRACE-based HAM and GAO.

## 1. INTRODUCTION

It is commonly known that for time scales of a few years or shorter, the main contributors to polar motion (PM) excitation are variations in global mass distribution of atmosphere, ocean and continental hydrosphere. The atmospheric and oceanic contributions have been well-established (Gross et al. 2003; Nastula et al. 2007; 2009) but HAM is believed to be the main source of uncertainties in PM excitation. It was shown in recent researches that compared to Hydrological Angular Momentum (HAM) estimations obtained from either hydrological or climate models, GRACE-based HAM functions were in better agreement with hydrological signal in observed PM excitation (Nastula et al. 2019; Seoane et al. 2011; Śliwińska et al. 2019).

Recently, the official GRACE data centres have been released new GRACE RL06 solutions and the first efforts to evaluate these data have been made in the work of (Göttl et al. 2018). That paper showed that both the consistency between particular solutions and the agreement between HAM and GAO have increased when applying the newly processed GRACE data.

A common method to describe PM excitation is the use of two equatorial components of this function,  $\chi_1$  and  $\chi_2$ . However, the polar motion excitation exhibits two circular terms: retrograde (clockwise) and prograde (counter-clockwise). In previous works, the PM excitation was generally decomposed into prograde and retrograde terms but at one fixed frequency. In this study, we considered the total prograde ( $\chi_P$ ) and retrograde ( $\chi_R$ ) parts of PM excitation function. We reconstructed these terms in time domain from  $\chi_1$  and  $\chi_2$  with the use of Complex Fourier Transform (CFT) (Bizouard 2016). The circular terms of investigated series were then separated into seasonal and non-seasonal oscillations.

The objective of this study was to consider what the new GRACE RL06 solutions might contribute to the understanding of residual PM excitations as observed by space geodesy techniques. Here, we validated HAM series from the new GRACE RL06 and from previous GRACE RL05 data, using observed hydrological signal in PM excitation, derived from precise measurements of pole

coordinates (geodetic residuals, GAO). The GRACE estimations of HAM were also compared with the HAM from Land Surface Discharge Model (LSDM).

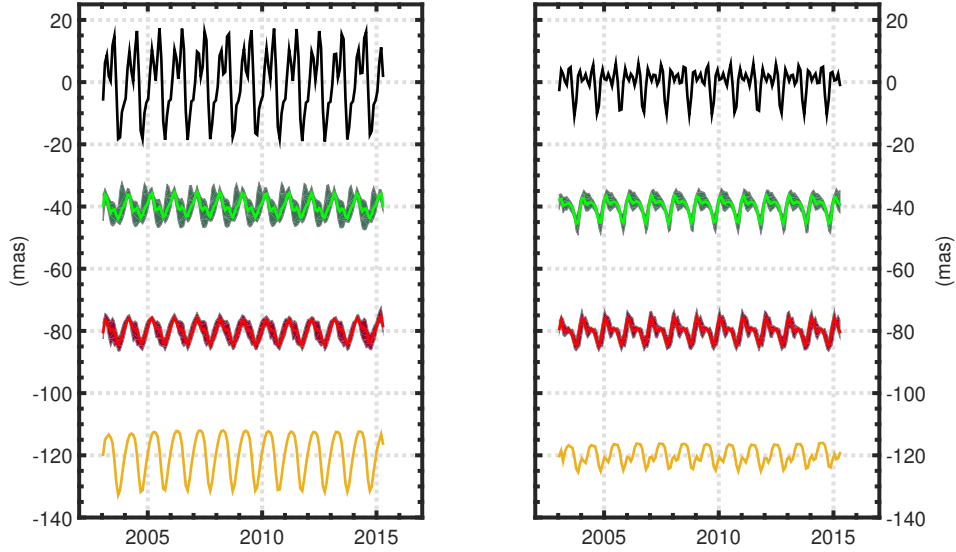


Figure 1: Retrograde (left) and prograde (right) parts of the seasonal HAM variation. Black line: GAO. Green and red lines: old and new averaged GRACE solutions respectively with the range between minimum and maximum values of the 5 individual solutions. Yellow line: LSDM model.

## 2. DATA SETS

### 2.1 Geodetic residuals (GAO)

The  $\chi_1$  and  $\chi_2$  components of the observed geodetic PM excitation function (Geodetic Angular Momentum, GAM) can be computed from observed coordinates ( $x$ ,  $y$ ) of the Earth pole which are routinely delivered as daily C04 series of Earth Orientation Parameters (EOP). In order to separate hydrology-related effects from GAM, the atmosphere and ocean angular momentum should be removed (AAM and OAM functions, respectively). The resulting residual series are denoted as geodetic residuals (GAO). In this study, GAM, obtained from the EOP 14 C04 series, were taken from the International Earth Rotation and Reference Systems Service (IERS) website (<https://www.iers.org/>). For mass terms of atmosphere and ocean, we used GAC JPL RL06 time series of  $\Delta C_{21}$ ,  $\Delta S_{21}$  coefficients of the GRACE non-tidal atmosphere and ocean de-aliasing data, available from <https://podaac-tools.jpl.nasa.gov/drive/files/allData/grace/L2/JPL/RL06>. Motion terms of AAM were computed by the GFZ from the European Centre for Medium-range Weather Forecasts (ECMWF) model and accessed from <ftp://esmdata.gfz-potsdam.de/./EAM/>. For motion terms of OAM, we used the series provided by GFZ and computed from Max Planck Institute Ocean Model (MPIOM).

### 2.2 HAM functions from GRACE

Here, we evaluated monthly GRACE satellite-only models (GSM), also denoted as GRACE Level-2 data. In order to compute HAM, we converted  $\Delta C_{21}$ ,  $\Delta S_{21}$  coefficients of the geopotential into  $\chi_1$  and  $\chi_2$  equatorial components of mass-related PM excitation function, based on formulas given in (Gross 2015). In this paper, we used the GRACE GSM fields provided by five different pro-

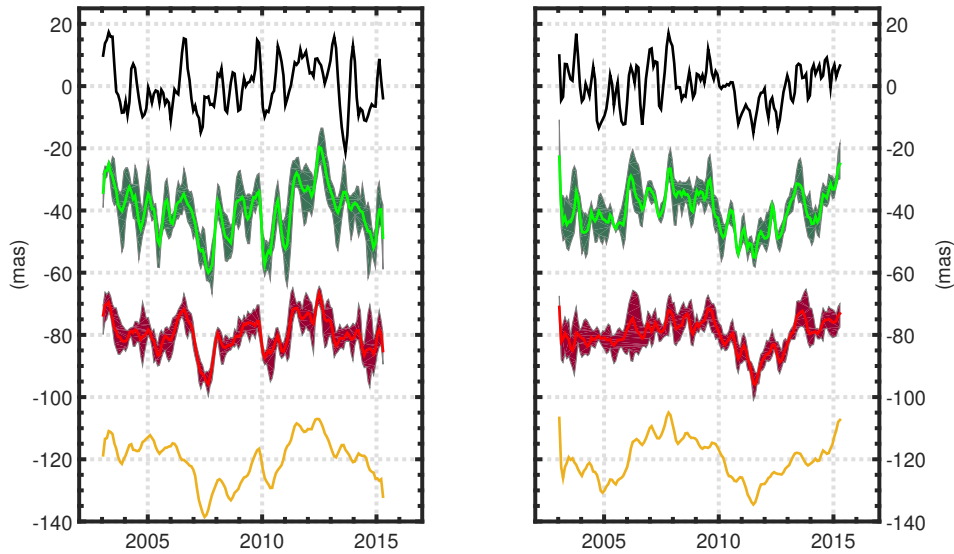


Figure 2: Retrograde (left) and prograde (right) parts of the non-seasonal HAM variation. Black line: GAO. Green and red lines: old and new averaged GRACE solutions respectively with the range between minimum and maximum values of the 5 individual solutions. Yellow line: LSDM model.

cessing centres: Center for Space Research (CSR RL05 and CSR RL06 solutions), Jet Propulsion Laboratory (JPL RL05 and JPL RL06 solutions), GeoForschungsZentrum (GFZ RL05 and GFZ RL06 solutions), Centre National d'Études Spatiales (CNES RL03 and CNES RL04 solutions), Institute of Theoretical Geodesy and Satellite Geodesy of the Graz University of Technology (ITSG 2016 and ITSG 2018 solutions).

### 2.3 HAM and SLAM functions processed by GFZ

We also considered HAM computed from the Land Surface Discharge Model (LSDM) and provided by GFZ (<ftp://esmdata.gfz-potsdam.de/./EAM/>). It should be kept in mind that both GRACE and GAO include barystatic sea level changes due to inflow of water from lands into the oceans (sea-level angular momentum, SLAM) but SLAM is not included in hydrological models. Therefore, to make LSDM-based HAM more comparable with GAO and GRACE estimates, we added SLAM to it. These SLAM series are also provided by the GFZ.

## 3. RESULTS

Figure 1 compares the prograde and retrograde values of seasonal HAM for the GRACE RL05 and RL06 averaged solutions. For each averaged values, we display the range between minimum and maximum values of the 5 GRACE individual solutions, mentioned above. Time series of GAO and HAM from the LSDM model (with SLAM added) are provided for comparison. It is clear that updating some background models and processing algorithms in the GRACE RL06 data resulted in increased compatibility of HAM between solutions from different data centres (indicated by reduced range), especially for the  $\chi_R$  term. Notably, the  $\chi_R$  part for the GRACE-based mean HAM data underestimated seasonal variations of both GAO and LSDM-based HAM. Figure 2 replicates Figure 1 but for the non-seasonal variations. It showed that non-seasonal variations were characterized by bigger amplitudes than seasonal ones, which was especially visible for GRACE data. With the new GRACE RL06 solutions, different estimations of HAM were more similar to each other but

visible discrepancies were still present. Nevertheless, the HAM from the mean of all new GRACE solutions revealed to be more consistent with GAO and LSDM-based HAM than the HAM from any single GRACE solution. In order to assess the variability of analysed time series, we computed their standard deviation (STD), shown in Table 1. For seasonal variations, the  $\chi_P$  and  $\chi_R$  parts reveal rather similar STD within each GRACE solution. Notably, almost all GRACE solutions underestimate the STD of HAM (except  $\chi_R$  for JPL RL05), and this was more evident for the  $\chi_R$  term. In terms of non-seasonal changes, the  $\chi_R$  circular term variation appeared to be stronger than the  $\chi_P$  term for most of the HAM series from old GRACE RL05 series (CSR RL05, JPL RL05, ITSG 2016, CNES RL03, except GFZ RL05), as indicated by the STD values (Table 1). For new GRACE RL06 data,  $\chi_R$  is stronger than  $\chi_P$  for HAM from CSR RL06, JPL RL06 and CNES RL04. GAO and HAM computed using LSDM are also characterized by biggest STD values for  $\chi_R$ . In order to analyse the agreement between different HAM series and GAO, we computed correlation coefficients (Table 2) and relative explained variances (Table 3). The relative explained variances were computed using formulae shown in Śliwińska et al. 2020. Table 2 showed that for seasonal oscillations, the CSR RL06 solution provided the highest correlation of HAM with GAO (0.87) for the  $\chi_R$  term, while the best result for the  $\chi_P$  part was obtained for CNES RL03 and CNES RL04 (0.74 and 0.73 respectively). The highest relative explained variance was obtained for CSR RL06 in  $\chi_R$  (51%) and for CNES RL03 and CNES RL04 in  $\chi_P$  (49% and 52%, respectively). Notably, the HAM function obtained from LSDM revealed a very good agreement with the GAO series but only pertaining to the retrograde part (correlation coefficient of 0.74 and relative explained variance of 54%).

Table 1: Standard deviation of retrograde and prograde terms of GAO and HAM time series for seasonal and non-seasonal variation. The values are given in mas

Series	Seasonal		Non-seasonal	
	$\chi_R$	$\chi_P$	$\chi_R$	$\chi_P$
GAO	10.24	4.35	8.00	6.83
CSR RL05	3.29	3.08	8.20	7.37
CSR RL06	3.82	3.80	6.43	5.80
JPL RL05	4.95	4.69	11.83	6.49
JPL RL06	3.14	3.00	6.35	5.69
GFZ RL05	3.31	2.77	8.68	8.76
GFZ RL06	2.36	2.42	5.96	6.05
CNES RL03	2.73	2.22	8.12	7.71
CNES RL04	2.86	2.64	7.15	6.13
ITSG 2016	2.48	1.94	9.02	6.94
ITSG 2018	2.95	3.14	5.65	5.84
LSDM	6.75	2.72	7.20	6.61

In terms of non-seasonal HAM changes, the best correlation agreement with GAO for both  $\chi_P$  and  $\chi_R$  terms was observed for CSR RL06 (0.66 and 0.68 for  $\chi_R$  and  $\chi_P$ , respectively) and ITSG 2018 data (0.64 and 0.59 for  $\chi_R$  and  $\chi_P$ , respectively), and the highest relative explained variance was obtained for CSR RL06 (42% and 44% for  $\chi_R$  and  $\chi_P$ , respectively) and ITSG 2018 solutions (40% and 28% for  $\chi_R$  and  $\chi_P$ , respectively). For  $\chi_P$ , LSDM-based HAM provided results comparable with those obtained for CSR RL06 and ITSG 2018.

## 4. CONCLUSIONS

In this study, we decomposed equatorial components of HAM ( $\chi_1$  and  $\chi_2$ ) into prograde and retrograde circular terms ( $\chi_P$  and  $\chi_R$ ), using CFT. We evaluated  $\chi_P$  and  $\chi_R$  components of HAM

Table 2: Correlation coefficients of retrograde and prograde parts of seasonal and non-seasonal variation between GAO and different HAM. The critical value of the correlation coefficient for 25 independent points and a confidence level of 0.95 was 0.34. The standard error of the difference between two correlation coefficients for 25 independent points was 0.30

Series	Seasonal		Non-seasonal	
	$\chi_R$	$\chi_P$	$\chi_R$	$\chi_P$
CSR RL05	0.84	0.48	0.50	0.51
CSR RL06	0.87	0.62	0.66	0.68
JPL RL05	-0.57	0.31	0.45	0.56
JPL RL06	-0.07	0.08	0.50	0.35
GFZ RL05	0.67	0.40	0.42	0.67
GFZ RL06	0.84	0.58	0.30	0.48
CNES RL03	0.63	0.74	0.49	0.53
CNES RL04	0.60	0.73	0.48	0.56
ITSG 2016	0.80	0.28	0.49	0.57
ITSG 2018	0.68	0.64	0.64	0.59
LSDM	0.74	0.11	0.35	0.64

Table 3: Percentage of variance in GAO explained by HAM functions for retrograde and prograde parts of seasonal and non-seasonal variation. The values are given in %

Series	Seasonal		Non-seasonal	
	$\chi_R$	$\chi_P$	$\chi_R$	$\chi_P$
CSR RL05	43	18	-3	-6
CSR RL06	51	32	42	44
JPL RL05	-78	-50	-87	16
JPL RL06	-13	-37	16	-12
GFZ RL05	33	11	-26	8
GFZ RL06	34	34	-11	7
CNES RL03	27	49	-4	-8
CNES RL04	26	52	6	21
ITSG 2016	33	5	-15	13
ITSG 2018	31	41	40	28
LSDM	54	-25	-19	29

obtained from GRACE RL05 and RL06 series and from LSDM hydrological model by comparing them with hydrological signal confused with PM excitation residual (GAO). In contrast to  $\chi_1$  and  $\chi_2$  representation, where we observed significantly better results for  $\chi_2$  than for  $\chi_1$  component (see e.g. Nastula et al 2019, Śliwińska et al. 2019, 2020), the consistency with GAO was at the similar level for both  $\chi_R$  and  $\chi_P$ . The new GRACE solutions leads to an better consistency between  $\chi_R$  and  $\chi_P$ .

Despite different methods of representation, our general conclusions are similar to those drawn in works dedicated to  $\chi_1$  and  $\chi_2$  analyses. With the new GRACE data, the consistency between different solutions has been increased. HAM from the new RL06 GRACE data were more smoothed (smaller amplitudes and standard deviation) compared to HAM from RL05. The new GRACE solutions provide better correlation and variance agreement with observed PM excitation than the previous GRACE data. Despite improved correlation agreement with reference data, there is still no satisfactory amplitude and variance compatibility. For most of the oscillations considered, the highest agreement with reference data was obtained for CSR RL06 and ITSG 2018 solutions. The highest results improvement was detected for JPL.

We also noted that the HAM obtained from LSDM model is significantly correlated with GAO for the non-seasonal prograde and seasonal retrograde parts.

**Acknowledgements.** This research was funded by National Science Centre, Poland (NCN), grant number 2018/31/N/ST10/00209.

## 5. REFERENCES

- Bizouard, C., 2016, "Elliptic polarisation of the polar motion excitation", *J. Geodesy* 90(2), pp. 179–188, doi:10.1007/s00190-015-0864-7.
- Göttl, F., Schmidt, M., Seitz, F., 2018, "Mass related excitation of polar motion: an assessment of the new RL06 GRACE gravity field models", *Earth Planets Space* 70(1), doi:10.1186/s40623-018-0968-4.
- Gross, R., 2015. "Theory of earth rotation variations". Sneeuw, N., Novak, P., Crespi, M., Sanso, F. (Eds.), VIII Hotine-Marussi Symposium on Mathematical Geodesy, doi:10.1007/1345\_2015\_13S.
- Gross, R.S., Fukumori, I., Menemenlis, D., 2003, "Atmospheric and oceanic excitation of the Earth's wobbles during 1980-2000", *J. Geophys. Res. (Solid Earth)*, 108(B8), 2370, doi:10.1029/2002JB00214.
- Nastula, J., Wińska, M., Śliwińska, J., Salstein, D., 2019, "Hydrological signals in polar motion excitation - Evidence after fifteen years of the GRACE mission", *J. Geodyn.* 124, pp. 119–132, doi:10.1016/j.jog.2019.01.014
- Nastula, J., Ponte, R.M., Salstein, D.A., 2007, "Comparison of polar motion excitation series derived from GRACE and from analyses of geophysical fluids", *Geophys. Res. Lett.* 34(11), 2-7, doi:10.1029/2006GL028983.
- Nastula, J., Salstein, D.A., Kolaczek, B., 2009, "Patterns of atmospheric excitation functions of polar motion from high-resolution regional sectors", *J. Geophys. Res.* 114(B4), B04407, doi:10.1029/2008JB005605.
- Seoane, L., Nastula, J., Bizouard, C., Gambis, D., 2011, "Hydrological excitation of polar motion derived from GRACE gravity field solutions", *International Journal of Geophysics*, doi:10.1155/2011/174396.
- Śliwińska, J., Nastula, J., Dobslaw, H., Dill, R., 2020, "Evaluating gravimetric polar motion excitation estimates from the RL06 GRACE monthly-mean gravity field models", *Remote Sensing* 12(6), doi:10.3390/rs12060930.
- Śliwińska, J., Wińska, M., Nastula, J., 2019, "Terrestrial water storage variations and their effect on polar motion", *Acta Geophys.* 67(1), pp. 17–39, doi:10.1007/s11600-018-0227-x.